Journal id: GGAF_A_186840

Corresponding author: C. C. Lim

Title: Statistical equilibrium distributions of baroclinic vortices in a rotating two-layer model at low Froude numbers

NO QUERIES

Geophysical and Astrophysical Fluid Dynamics,
Vol. 100, No. 6, Month?? 2006, 1–22

Taylor & Francis
Taylor & Francis Group

Statistical equilibrium distributions of baroclinic vortices in a rotating two-layer model at low Froude numbers

SYED M. ASSAD† and CHJAN C. LIM*‡

†Physics Department, National University of Singapore, Singapore
‡Mathematical Sciences, Rensselaer Polytechnic Institute,
Troy, NY 12180, USA

(*Received 27 September 2005; in final form 1 June 2006*)

The point-vortex equilibrium statistical model of two-layer baroclinic quasigeostrophic vortices in an unbounded *f*-plane is examined. A key conserved quantity, angular momentum, serves to confine the vortices to a compact domain, thereby justifying the statistical mechanics model, and also eliminating the need for boundary conditions in a practical method for its resolution. The Metropolis method provides a fast and efficient algorithm for solving the mean field non-linear elliptic PDEs of the equilibrium statistical theory. A verification of the method is done by comparison with the exact Gaussian solution at the no interaction limit of zero inverse temperature. The numerical results include a geophysically and computationally relevant power law for the radii at which the most probable vortex distribution is non-vanishing: For fixed total circulation, and fixed average angular momentum, the radii of both layers are proportional to the square root of the inverse temperature β. By changing the chemical potentials μ of the runs, one is able to model the most probable vorticity distributions for a wide range of total circulation and energy. The most probable vorticity distribution obtained at low positive temperatures are consistently close to a radially symmetric flat-top profiles. At high temperatures, the radially symmetric vorticity profiles are close to the Gaussian distribution.

Keywords: Rotating two-layer model; Statistical mechanics; Monte Carlo simulation; Mean field theory

1. Introduction

In the equilibrium statistical mechanics model developed by DiBattista and Madja (2001) for two-layer quasi-geostrophic vortices in an unbounded *f*-plane (Hogg and Stommel 1985a, b, Legg and Marshall 1993) the rotational invariance of the Hamiltonian and domain give rise to an angular momentum constraint. This key quantity confines the most probable vorticity distribution to a finite region and justifies doing equilibrium statistical mechanics in an unbounded plane. In the same paper, they derived the mean field equations for this model, which was then solved numerically

*Corresponding author. Email: limc@rpi.edu

Geophysical and Astrophysical Fluid Dynamics
ISSN 0309-1929 print: ISSN 1029-0419 online © 2006 Taylor & Francis
http://www.tandf.co.uk/journals
DOI: 10.1080/03091920600869120

using an iterative algorithm. In this article we shall approach the same problem using a Monte Carlo (MC) algorithm. Thus, we avoid making any assumptions about the exactness of the mean field theory (which is likely true although not proved). At the same time, we also do not make any assumptions on the prior distributions governing the small scales in the problem. This is a necessary step within the framework of the maximum entropy mean field theory used in DiBattista and Madja (2000, 2001). Nonetheless, we find results that are consistent with their approach.

Extensive numerical results on the vortex dynamics of the rotating two-layer model have been reported in several papers (Gryanik 1983, Hogg and Stommel 1985a,b, Legg and Marshall 1998, Held *et al*. 1995, Legg *et al*. 1996, Legg and Marshall 1993, Marshall and Schott 1999). Some of the qualitative properties of long-lived coherent structures in two-layer quasi-geostrophic flows are confirmed by DiBattista and Madja (2001).

The vortices in the model that we are studying interact via a Hamiltonian H subject to a constraint on their angular momentum Γ. The explicit forms of H and Γ are given in equations (3) and (4), respectively. These two contributions to the vortex interactions are grouped together to give the augmented Hamiltonian $E = H + (\mu/\beta)\Gamma$. In statistical mechanics, the quantity μ is traditionally called chemical potential and β is called the inverse temperature: $\beta = 1/T$. We remark that T is the statistical temperature and not the physical molecular temperature of the fluid. This T measures the amount of kinetic energy in the large scale flows while the molecular temperature would measure the amount of kinetic energy per molecule in the Maxwell–Boltzmann equilibrium distribution.

The ratio μ/β characterises the strength of the interaction contributions from angular momentum term relative to that from the Hamiltonian term. For example, when this ratio is large, the angular momentum plays a dominant role compared to the Hamiltonian. When the ratio is small, the Hamiltonian term has a greater contribution to the vortex interactions as compared to the angular momentum term.

In this article, we are interested in the coarse-grained vortex configurations at statistical equilibrium in the low Froude number case in problems with a definite barotropic bias due, for instance, to preconditioning by open ocean gyres. Instead of maximising the information-theoretic relative entropy in a mean field theory (as in DiBattista and Majda 2000), we perform direct statistical sampling of the related Gibbs ensemble. The equilibrium smooth vortex we find have symmetric and concentric (with respect to the two layers) distributions, that is indicative of a cold baroclinic core, consistent with the results in DiBattista and Madja (2000).

In other words, for positive temperatures, we search for the vortex distributions that would minimise the Helmholtz free energy: $F = E - TS$, where S is the entropy of the vortex system. Please note the abuse of notations. Here E refers to the augmented energy of a vortex configuration obtained by the action of the augmented Hamiltonian operator (also denoted as E) on the vortex configuration. The temperature of the system T characterises the relative importance of the two quantities E and S. In some sense, the temperature characterises the strength of the vortex interactions. At high temperatures, to minimise the free energy, the equilibrium vortex configuration would be a high entropy configuration. Here the augmented energy has little contribution to the free energy. At the other extreme, when the temperature is low, the energy term plays a more dominant role. The vortex system would favour a low energy configuration and its entropy does not have much effect on the equilibrium configuration.

In the M-C simulations reported here we run the numerical experiments over a wide range of β and μ, with two aims in mind, namely, (a) to find phase transitions or to exclude them which is the case here and (b) more importantly, to find relationships between bulk variables or order parameters such as the containment radii of the equilibrium vorticity distributions and β and μ.

The main aim of this article is to report a new power law for the radial extent of the equilibrium vorticity distributions: For fixed total circulations and fixed average angular momentum, the radial extent of both layers are proportional to the square root of the inverse temperature. This power law is important in the geophysical context not only because it further justifies the statistical mechanics approach on an unbounded f-plane, but also because it provides a useful explicit relation between mean angular momentum, total circulation and the radial extent of the vorticity in each layer. Some of the specific geophysical consequences of this power law are discussed in the conclusion of the article.

This power law is also significant for a purely computational reason, namely, it allows us to effectively solve the mean field equations for the rotating two-layer model on disks of any radii, just by changing the values of the mean angular momentum and total circulation in the Monte Carlo algorithm. The point-vortex MC method provides an economical approach to solving these mean field equations. This algorithm had previously been used in the study of equilibrium statistical mechanics of vortices in the plane (Assad and Lim 2005, Lim and Assad 2005) and on the sphere (Lim and Nebus 2004). In this article, we extend its use to an unbounded two layer baroclinic point vortex model. We verify the method by providing exact solutions of the model at infinitely high temperatures and comparing the numerical output to these results. We stress, however, that the results reported here are strictly of a statistical equilibrium type. The results represent the steady-state structures of the fluid. The MC method cannot capture the dynamics of an evolving fluid.

In equilibrium statistical physics, all the relevant physical information is in the coarse-grained macrostate (smooth super vortex) rather than in the much more detailed microstates. On the other hand, the geophysically interesting case where several long-lived clusters of individual vortices evolve dynamically over time scales that are long compared to the relaxation time in our experiments, is likely to be a non-equilibrium phenomena and not strictly within the scope of the MC methods used here. In another paper, these quasi-steady clustered vortex states of the associated N-body Hamiltonian equations are related to KAM tori. The non-equilibrium properties of these clustered vortex states requires further study, using a dynamical systems (N-body problem) approach rather than the Markov Chain MC method used here.

This article is organised as follows: in section 2, we collect all the equations and mention some of their consequences. Section 3 describes the MC algorithm. Section 4 compares the Monte Carlo algorithm with the exact solution of the vorticity equations at inverse temperature $\beta = 0$. The numerical results gathered by the MC simulations for positive and negative β are presented in sections 5 and 6, respectively.

2. Two-layer quasi-geostrophic vorticity equations

DiBattista and Madja (2001) present a comprehensive discussion on the two-species point vortex model of the two-layer quasi-geostrophic vorticity equations. In this

model, the stratified fluid which is permitted to evolve in an unbounded plane, is partitioned into two thin slabs, each of constant depth, density and temperature. We shall not reproduce their discussions here, instead we collect only the necessary equations for our modelling purposes. The reader is referred to several relevant papers describing the geophysical origins of this theory (Gryanik 1983, Hogg and Stommel 1985a,b, Legg and Marshall 1993, Held *et al*. 1995, Legg *et al*. 1996, Legg and Marshall 1998, Marshall and Schott 1999, Lim and Majda 2001).

The two-layer quasi-geostrophic vorticity model gives rise to the following conserved quantities:

$$Q_A = \int_{R^2} q_A, \quad Q_B = \int_{R^2} q_B, \tag{1, 2}$$

$$H = -\frac{1}{2}\sum_{j=A,B}\int_{R^2}\psi_j q_j, \quad \Gamma = \sum_{j=A,B}\int_{R^2} q_j|\mathbf{x}^2|. \tag{3, 4}$$

$q_A(\mathbf{x})$ and $q_B(\mathbf{x})$ are the vortex density of the upper and lower layers, respectively. In this article, we shall only consider positive vorticity, $q_i(\mathbf{x}) > 0$ for all $\mathbf{x}$. ψ_A and ψ_B are the stream functions on the upper and lower layers, respectively. They are coupled through the relations

$$q_A = \Delta\psi_A - (F\psi_A - F\psi_B) \quad \text{and} \quad q_B = \Delta\psi_B + (F\psi_A - F\psi_B).$$

where Δ denotes the horizontal Laplacian operator and F is related to the Rossby radius L_ρ by

$$F = 1/L_\rho^2.$$

Conserved quantities (1) and (2) follow from the separately conserved circulation of each layer. The quantity H is the pseudo-energy of the vortex system. Γ is the angular momentum which is conserved as a consequence of the rotational invariance of the infinite plane.

The important role of angular momentum in the confinement of the baroclinic vortices to a bounded region, highlighted in DiBattista and Madja (2001), is based on a rigorous mathematical result for the rotating two-layer model (Lim and Majda 2001) which gives a necessary and sufficient condition for boundedness of baroclinic vortex dynamics. The conditions for the existence of robust, localised coherent vortical structures in the long-time dynamics of the rotating two-layer model are in the form of a non-zero sum of total circulation over the two layers in the model. They should be compared to the geophysically extent conditions that are found in localised open ocean convection sites where a preconditioned ocean gyre (often due to prevailing winds) provides the non-zero sum condition on the circulations in the rotating two-layer model. A non-zero sum condition is built into the MC simulations for the explicit purpose of such a comparison with geophysically relevant data.

2.1. *Point vortex model*

To allow numerical simulations of the two-layer quasi-geostrophic model, we need to discretise the vortex field. We represent q_A and q_B with N discrete point vortices in each layer. That is, there are $2N$ point vortices, N of which belong to the upper layer, each with vorticity $\omega_A = Q_A/N$; and the remaining N belong to the lower layer, each having vorticity $\omega_B = Q_B/N$. We call the vortices representing the upper layer as species A and those representing the lower layer as species B.

This representation automatically ensures that the total circulation of each species is separately conserved. Using point vortices to represent a continuous density distribution leads to a delta-function-like vorticity profile. The probability of locating a point vortex in a certain finite area near $\mathbf{x}$ can be interpreted as the vortex density $q(\mathbf{x})$ in that area. And as $N \to \infty$, we expect this density to converge to the continuous vorticity densities q_A and q_B.

The discretised version of the pseudo-energy (3) would be

$$\begin{aligned} H = &-\frac{\omega_A^2}{2}\sum_{i\neq j}\left[G_B(\mathbf{x}_i,\mathbf{x}_j) + G_T(\mathbf{x}_i,\mathbf{x}_j)\right] \\ &-\frac{\omega_B^2}{2}\sum_{m\neq n}\left[G_B(\mathbf{x}_m,\mathbf{x}_n) + G_T(\mathbf{x}_m,\mathbf{x}_n)\right] \\ &-\frac{\omega_A\omega_B}{2}\sum_{i,m}\left[G_B(\mathbf{x}_i,\mathbf{x}_m) - G_T(\mathbf{x}_i,\mathbf{x}_m)\right] \end{aligned} \tag{5}$$

and that for the angular momentum (4)

$$\Gamma = \omega_A\sum_i \mathbf{x}_i^2 + \omega_B\sum_m \mathbf{x}_m^2. \tag{6}$$

In the above, the subscripts i and j denote vortices of the upper layer while subscripts m and n denote vortices in the lower layer. G_B and G_T are the Green's functions for the barotropic, $(q_A + q_B)/2$ and baroclinic, $(q_A - q_B)/2$ vorticity field, respectively. They are given by

$$\begin{aligned} G_B(\mathbf{x}_i,\mathbf{x}_j) &= \frac{1}{2\pi}\log|\mathbf{x}_i - \mathbf{x}_j|, \\ G_T(\mathbf{x}_i,\mathbf{x}_j) &= -\frac{1}{2\pi}\mathrm{K}_0\left(\sqrt{2F}|\mathbf{x}_i - \mathbf{x}_j|\right). \end{aligned}$$

K_0 is the zeroth order modified Bessel function of the second kind.

2.2. *Properties of pseudo-energy H*

In this section, we shall examine the action of H in equation (5) on a two vortex system.

For two vortices far apart, the K_0 component of their interaction vanishes. H then does not distinguish between the two layers. Hence for a vortex system where the number of vortices is small, and the distance between vortices is large, the system

then effectively behaves like a single-layer system with total vorticity $N(\omega_A + \omega_B)$. Also the pseudo-energy $H(r_{ij})$ would decrease when r_{ij} increases.

Next, consider two vortices close to each other such that the effects of K_0 cannot be disregarded. Now a vortex from the upper layer sees other vortices from the same layer differently as those from the lower layer. Hence we shall consider the same layer interaction and the different layer interaction separately.

In the *same layer*, both the log and K_0 terms of the pseudo-energy would result in a lower pseudo-energy if the vortices are separated further apart:

$$H_{AA}(r_{ij}) = \frac{\omega_A^2}{4\pi}\left[-\log r_{ij} + \mathrm{K}_0\left(\sqrt{2F}r_{ij}\right)\right].$$

However between *different layers*, to lower the pseudo-energy, the log term would cause the vortices to repulse, while the K_0 term causes them to attract each other. Expanding the K_0 term as a Taylor series about the separation between the two vortices, $r_{im} = 0$, we get

$$\begin{aligned} H_{AB}(r_{im}) &= \frac{\omega_A\omega_B}{4\pi}\left[-\log r_{im} - \mathrm{K}_0\left(\sqrt{2F}r_{im}\right)\right] \\ &= \frac{\omega_A\omega_B}{4\pi}\left[\left(\gamma - \frac{1}{2}\log 2 + \frac{1}{2}\log F\right)\right. \\ &\quad \left. + \frac{r_{im}^2 F}{2}\left(\gamma - 1 - \frac{1}{2}\log 2 + \frac{1}{2}\log F + \frac{1}{2}\log r_{im}\right) + \mathrm{O}\left(r_{im}^4\right)\right]. \end{aligned}$$

Since $\log r_{im}$ is negative, we conclude that the two components act together to cause a net pseudo-energy term like $-r_{im}^2$. This produces a net repulsive potential between two vortices of different species.

So in all cases, the pseudo-energy term creates a repulsive potential that would cause two vortices to repulse each other. This can also be seen by observing that the gradient of $H(r)$ is always negative.

2.3. *Equilibrium statistical mechanics*

From the point of view of equilibrium statistical mechanics, the point vortices can take any accessible configuration, but each with a certain probability. The probability of a $2N$ vortex configuration $\mathbf{z}_N$ is given by (see appendix of DiBattista and Majda 2001)

$$P(\mathbf{z}_N) = \frac{\exp\{-\beta H(\mathbf{z}_N) - \mu\Gamma(\mathbf{z}_N)\}}{\int \exp\{-\beta H(\mathbf{z}_N) - \mu\Gamma(\mathbf{z}_N)\}\mathrm{d}\mathbf{z}_N}. \tag{7}$$

β and μ are the Lagrange multipliers associated with the conservation of H and Γ, respectively. When a vortex is located far from the origin, the quantity $\Gamma(\mathbf{z}_N)$ becomes large. From (7) we see that although the probability of a vortex being found far from the origin is non-zero (except when $\mu = \infty$), it is exponentially small.

General principles of equilibrium statistical mechanics state that the expected or mean values of the Lagrange multipliers are given by the corresponding derivatives

of the free energy with respect to the quantities associated with the multipliers, evaluated at the fixed values of these multipliers. For example, a given initial (and conserved) value H' of the pseudo-energy H in the physical system corresponds to a particular value β' of the inverse temperature for both the physical system and the energy reservoir it is attached to, and vice versa. The expected value of the energy H' would be the derivative of the free energy with respect to the inverse temperature β, evaluated at the value β'.

Since each vortex lives in a two-dimensional space, the whole model has $4N$ dimensions. To explicitly calculate the probability of each configuration $\mathbf{z}_N$ we need to evaluate the denominator of (7). This involves an integration over $4N$ dimensions. It is conceivable that one could attempt to calculate this quantity numerically by doing the following steps. First restrict each of the two-dimensional plane to a large enough domain. Second discretise this domain into a mesh of small finite areas, and finally add up all the contributions from all possible permutations of vortices in this discrete mesh. However, this direct calculation would require enormous computational power.

Instead, we proceed in a different direction. We use a MC algorithm to generate a Markov chain of states. And from this finite collection of states, we deduce the equilibrium statistical properties of the model.

3. Monte Carlo algorithm

The implemented MC algorithm is the standard Metropolis algorithm. The algorithm begins with $2N$ vortices, N of each type, placed randomly on the disk of arbitrary radius. The formulation of the model in terms of point vortices ensures the conservation of total circulation in each layer. While not strictly necessary, we set the number of vortices of species A equal to the number of vortices of species B in all the simulations. The simulation proceeds as follows.

Step 1: From the initial distribution, $\mathbf{Z}_N$, one vortex is picked randomly from the $2N$ vortices.

Step 2: This vortex is then displaced in a random direction by a fraction of a preset maximum displacement. We call this new distribution $\mathbf{Z}'_N$. This small displacement would cause the vortex distribution to have a new augmented energy

$$E(\mathbf{z}'_N) = \beta H(\mathbf{z}'_N) + \mu\Gamma(\mathbf{z}'_N).$$

Step 3: This new distribution will be accepted or rejected based on the following rule:

$$\begin{aligned} &\text{if } \exp(-\Delta E) > I, \quad \text{accept,} \\ &\text{otherwise,} \qquad\qquad\ \ \text{reject.} \end{aligned} \tag{8}$$

ΔE is the difference of augmented energy between the new distribution and the old distribution. I is a uniformly distributed number between 0 and 1. If the new distribution is accepted, set $\mathbf{z}_N = \mathbf{z}'_N$, and repeat step 1. Otherwise discard $\mathbf{z}'_N$ and repeat step 1

with a new random vortex and displacement. N cycles of the loop constitute one sweep. The loop is exited after a large enough predetermined number of sweeps is reached.

The initial distribution is allowed to evolve for 100,000 sweeps to relax, after which the simulation is sampled after every 50 subsequent sweeps.

At each sampled configuration, properties of the N vortices configuration like its energy, angular momentum and radial distribution was measured. The mean radial distribution for the whole run is then obtained by taking the average over all the sampled configurations.

In doing the MC simulations, we do not know in advance what the corresponding equilibrium pseudo-energy or angular momentum would be for a particular value of β and μ. What is done is that we do numerical simulations with a particular fixed value of β and μ. The mean pseudo-energy and the angular momentum corresponding to these values of β and μ are then inferred by calculating these quantities directly from the generated sampled configurations. By varying the values of β and μ in our simulations, we can sample the equilibrium states for a wide range of pseudo-energy and angular momentum.

These numerical simulations were carried out on a 2.2 GHz Intel Xeon processor computer with 1 GB memory. In all the simulations, we have set the Rossby radius to one.

4. Zero inverse temperature

We begin our discussions with the simplest case, $\beta = 0$. At zero inverse temperature, there is no Hamiltonian interaction between vortices. Essentially, each vortex in the system moves independently from the rest. With no interaction between vortices, there is no force that keeps them apart. The angular momentum however is still in effect, and it is easily seen that the lowest augmented energy state has $\Gamma = 0$ and $E = 0$. This is attained when all $2N$ vortices lie exactly on the origin.

In the MC algorithm, the decision to accept or reject a proposed move depends only on its resulting change in energy. And since at each move, only one vortex is displaced, the resulting change of energy is just

$$\mu\omega\left(r^2_{i\text{-new}} - r^2_{i\text{-old}}\right),$$

where ω is the vorticity of the displaced vortex. It does not depend on the positions of any of the other vortices.

For zero β, any move that brings a vortex closer to the origin would always result in a lower augmented energy, and consequently the move would be accepted.

4.1. *Barotropic flow*

The rotating two-layer model is termed barotropic when the vorticities of both layers are equal, $\omega_A = \omega_B$. In fact at $\beta = 0$, the vortex model is solvable. The probability of finding a vortex of strength ω at r (distance measured from the origin) would be

$$P(r) = \frac{\exp\left(-\mu\omega r^2\right)}{Z},$$

where μ is the Lagrange multiplier associated with the angular momentum. Z is a normalisation factor

$$Z = \int_{R^2} \exp\left(-\mu\omega r^2\right) = \frac{\pi}{\mu\omega}.$$

Hence the vorticity profile of a single vortex is then

$$q = \frac{\omega}{\pi L^2}\exp\left(-\frac{r^2}{L^2}\right), \tag{8}$$

where we have introduced

$$L^2 = \frac{1}{\mu\omega}.$$

This is a Gaussian distribution with standard deviation L. The expected angular momentum of the single vortex would be:

$$\left\langle \Gamma(q) \right\rangle = \int_{R^2} \omega r^2 P(r) = \frac{1}{\mu}. \tag{9}$$

The above equation (9) can also be obtained directly from $\left\langle \Gamma(q) \right\rangle = -\partial(\log Z)/\partial\mu$. In doing the MC simulations, we fix the Lagrange multiplier μ, and from there measure the energy of the system. However an alternative way of looking at it; from the usual method of Lagrange multiplier is that the angular momentum of the system is fixed at Γ. The Lagrange multiplier is then determined by substituting the solution (8) back into (6). Doing this we would again obtain the same results

$$\mu = \frac{1}{\Gamma}.$$

Having N identical vortices would result in a vorticity profile with the same spread, only N times stronger:

$$q^N = \frac{N\omega}{\pi L^2}\exp\left(-\frac{r^2}{L^2}\right). \tag{10}$$

The expected angular momentum of the system is N times greater than that of the single vortex

$$\left\langle \Gamma\left(q^N\right) \right\rangle = \frac{N}{\mu}. \tag{11}$$

We see from (11) that in the discrete case of N vortices, the angular momentum depends on the number of point vortices used to model the system. However for the angular

momentum quantity to be meaningful, it should only depend on the physical property of total circulation $Q = N\omega$. Only Q appears in the continuous model, N and ω were artificially introduced during the discretisation of the continuous vortex profile. The way to correct this would be to scale the Lagrange multipliers β and μ appropriately by a factor of N. But in this article, we shall not be concerned with the scaling of the multipliers. For here, we do not make any comparisons with varying N and only a few cases of different N will be discussed.

4.2. *Baroclinic flow*

With two species of different vorticity, the flow is called baroclinic. However at $\beta = 0$, the analysis above follows with little change. The most probable vortex profile would be two independent Gaussian profiles:

$$q_A^N = \frac{N\omega_A}{\pi L_A^2}\exp\left(-\frac{r^2}{L_A^2}\right), \quad q_B^N = \frac{N\omega_B}{\pi L_B^2}\exp\left(-\frac{r^2}{L_B^2}\right),$$

where

$$L_A^2 = \frac{1}{\mu\omega_A}, \quad L_B^2 = \frac{1}{\mu\omega_B}.$$

Table 1 gives a comparison of the vorticity profile obtained by the MC simulations using $N = 1$ with the exact results. 2×10^9 sweeps were used and a typical run takes about 1400 s.

Figure 1 shows the mean vorticity profile for $\mu = 2$. For this and all subsequent figures, we take radial symmetry of the profile to be given and plot only the radial variations. The kurtosis, β_2, of the profile was measured using:

$$\beta_2 = \frac{\mu_4}{\mu_2},$$

where μ_i is the i-th central moment. The discrete central moment is obtained from

$$\mu_i = \frac{\sum_j x_j r_j^i}{\sum_j x_j},$$

Table 1. Comparison of Monte Carlo with exact values for $\beta = 0$ with $N = 1$.

μ	Height	Standard deviation	$\langle\Gamma\rangle$	$\frac{N_\omega}{\pi L^2}$	L	$\frac{N_\omega}{\mu}$
1	0.3201081	0.996964	0.9792	0.3183	1	1
2	0.638957	0.705566	0.4982	0.6366	0.7071	0.5
3	0.958247	0.576113	0.3327	0.9549	0.5774	0.3333
4	1.2749	0.499584	0.2497	1.273	0.5	0.25

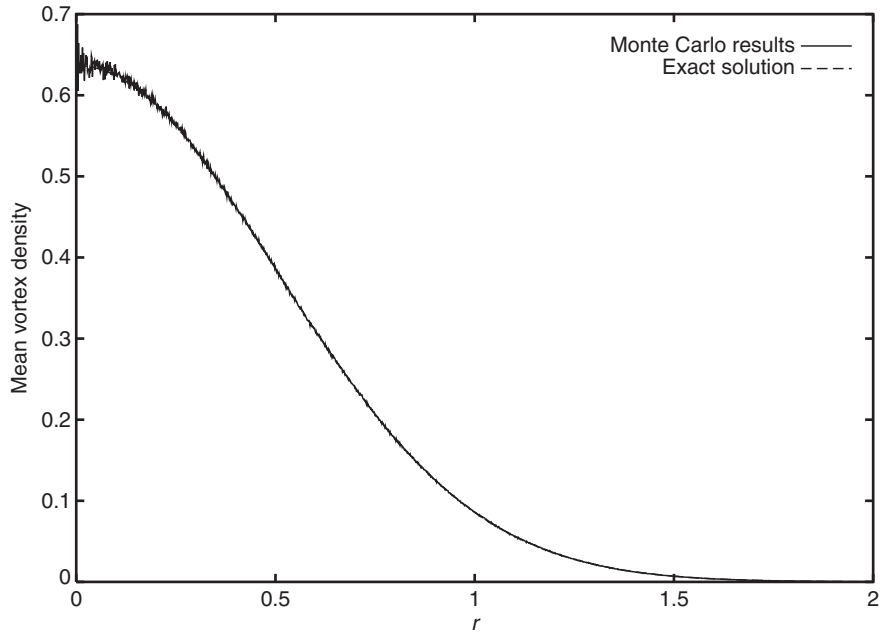

Figure 1. Comparison of the mean vortex density as obtained from the Monte Carlo simulations with the exact solution when $\omega = 1$, $\beta = 0$, $\mu = 2$, and $N = 1$. The two profiles coincide closely and are virtually indistinguishable. The Monte Carlo results were obtained from samples gathered after 2×10^9 sweeps. The Monte Carlo profile has a kurtosis of 3.0056, close to that of a true Gaussian.

where we have discretised the profile into a finite number of radial bins centred at a distance r_j away from the origin. x_j is the height of the radial profile at the j-th bin. The sum for the central moment is taken over all the non-zero radial bins.

In this figure, we see that the MC results closely match the exact results.

Repeating this experiment with bigger N gives similarly accurate results. The profiles obtained were similar Gaussians, with amplitudes as predicted by (10). These results shall not be presented here.

Only when $\beta = 0$, can we make such comparisons. Explicit solutions for other values of β are not known. In fact for $\beta = 0$, what is taking place is equivalent to a random walk.

5. Positive β

The next set of experiments deals with positive β. Figure 2 shows four simulations with $N = 60$, $\beta = 1$ and $\mu = 1$. ω_A is fixed at 1, while ω_B varies from 1 to 4. Each simulation involves five million sweeps that took approximately 33000 s. The vertical axis shows the vortex density of species B. The profile for species A have been scaled to match that of species B.

We see that when $\omega_A \neq \omega_B$, the two profiles differ; on average they are not equally mixed. Also when $\omega_A \neq \omega_B$, species A (having a lower circulation) are more concentrated in the central region. Its profile is closer to the Gaussian. Meanwhile, species

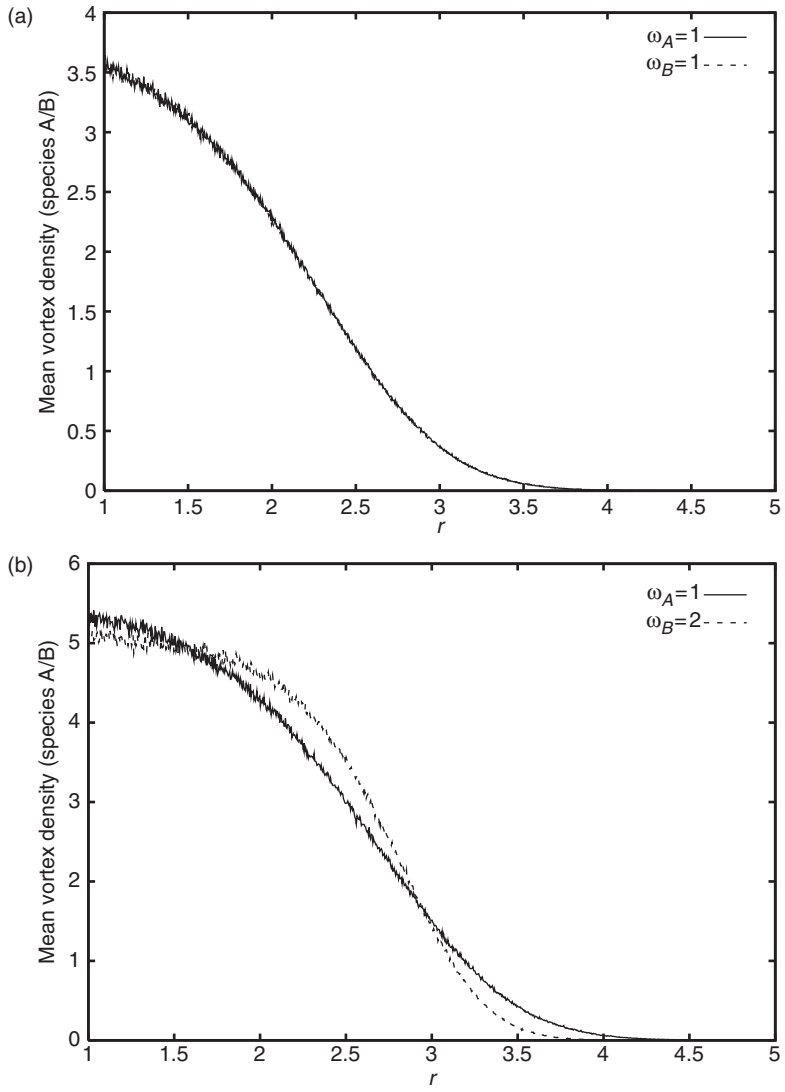

Figure 2. Vorticity profile for $N=60$, $\beta=1$, and $\mu=1$. $\omega_A=1$ in all four figures. (a) $\omega_B=1$, (b) $\omega_B=2$, (c) $\omega_B=3$, and (d) $\omega_B=4$.

365 B shows a flatter profile. This can also be seen in figure 3, which shows a typical Markov snapshot.

Table 2 gives the kurtosis values of the radial profiles.

As ω_B increases the vortex density profile of species B gradually flattens and its kurtosis approaches 1.8, the value for a uniform distribution. The density profile of 370 species A similarly flattens, even though its vorticity was unchanged at 1.

The vorticity profiles in figure 2 show that the equilibrium flow field is a 'smooth radially symmetric super vortex'. The typical instantaneous vortex distribution as shown in figure 3 offers a snapshot of this smooth super vortical field. Another way

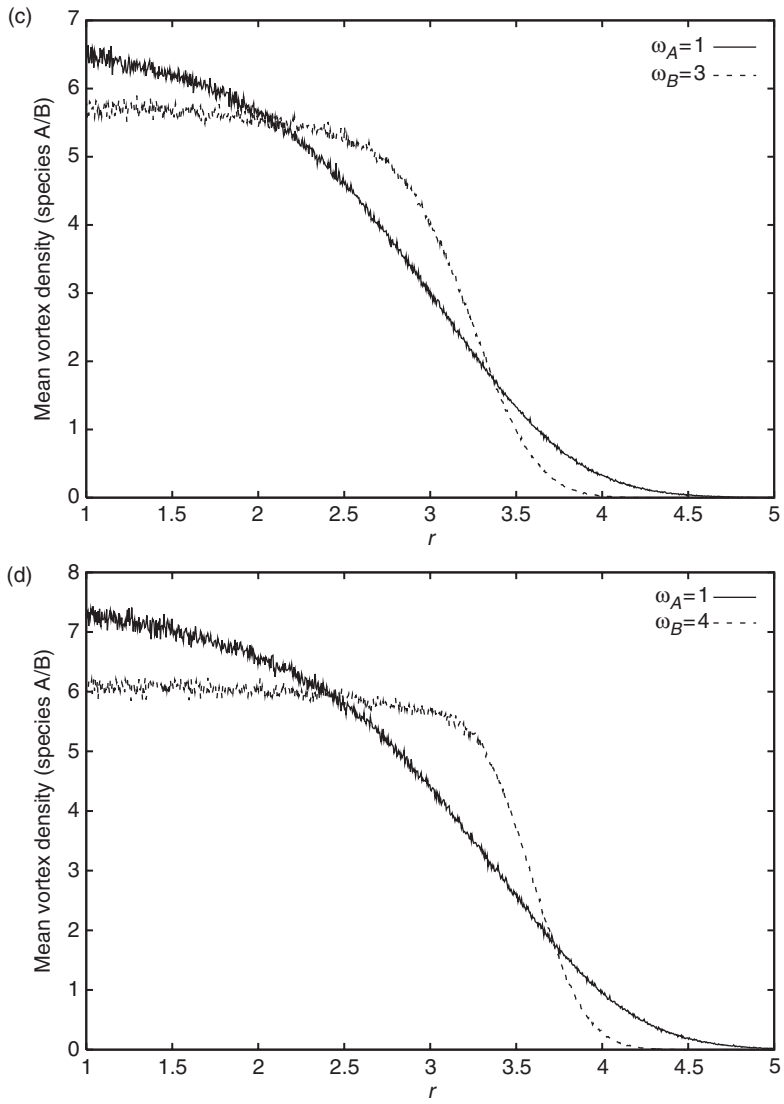

Figure 2. Continued.

of saying this is that the snapshot in figure 3 is a microstate of the coarse-grained or averaged vorticity field in figure 2. Indeed, after an initial period of approaching statistical equilibrium, the MC algorithm used 'mixes' or mathematically speaking, 'rearranges vortex parcels' within the smooth super vortical structure. The observed approach towards the same statistical equilibrium vorticity distribution from a wide range of initial vorticity distributions confirms that the unique equilibrium macrostate is not only the most probable one but it has overwhelming probability in the sense that the combined probability of all other macrostates is small in comparison. In other words, the MC simulations provide numerical evidence of a Large Deviations principle in this statistical two-layer baroclinic model.

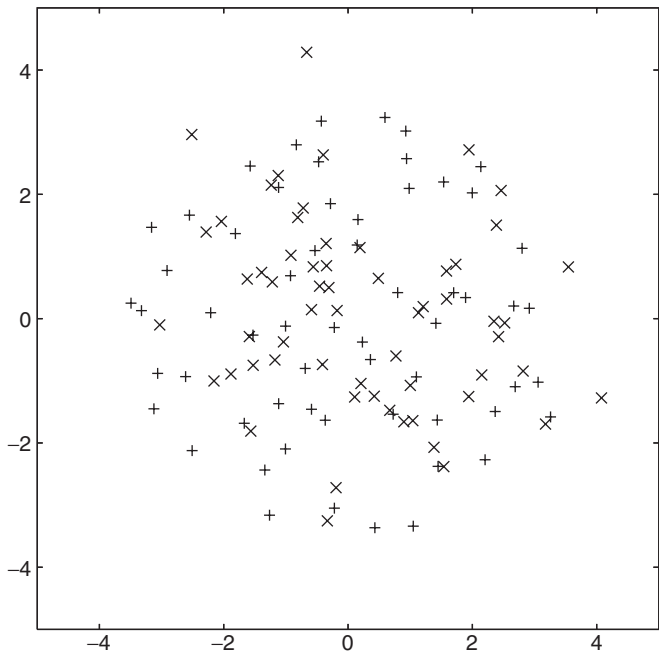

Figure 3. A typical vortex distribution snapshot with $N = 60$, $\beta = 1$, $\mu = 1$, $\omega_A = 1$ ('+'), and $\omega_B = 4$ ('×').

Table 2. Kurtosis values for the radial vorticity profiles.

ω_a	ω_b	Kurtosis A	Kurtosis B
1	1	2.2324	2.2396
1	2	2.1548	1.9798
1	3	2.1221	1.8920
1	4	2.0950	1.8560

In the next set of experiments, we keep ω_A, ω_B and μ fixed as β is varied. As β increases, we see the vortices of both species tend to a uniform distribution of the same radial extent. Figure 4 plots the distance of the furthest vortex from the origin in the vortex configuration, $R_{\max}$, against β for large values of β. It shows the relationship $R_{\max} \sim \sqrt{\beta}$.

DiBattista and Madja (2001) discovered a length scale L_A for the radial extent which is directly related to the angular momentum in the barotropic component, and to the $\beta = 0$ exact solution. The power law with exponent 1/2 in the quantity β/μ obtained here extends the relationship they found between L_A and angular momentum, to the $\beta > 0$ region. Through the power law's dependence on total circulations, inverse temperature β and chemical potential μ, we are also able to predict the radial extent of the equilibrium cold temperature and potential vorticity anomalies as a function of the mean kinetic energy and mean baroclinic angular momentum in the localised open ocean convection site. These quantities can be related back to the meteorological conditions that preconditioned the ocean site, such as the wind stress that caused the

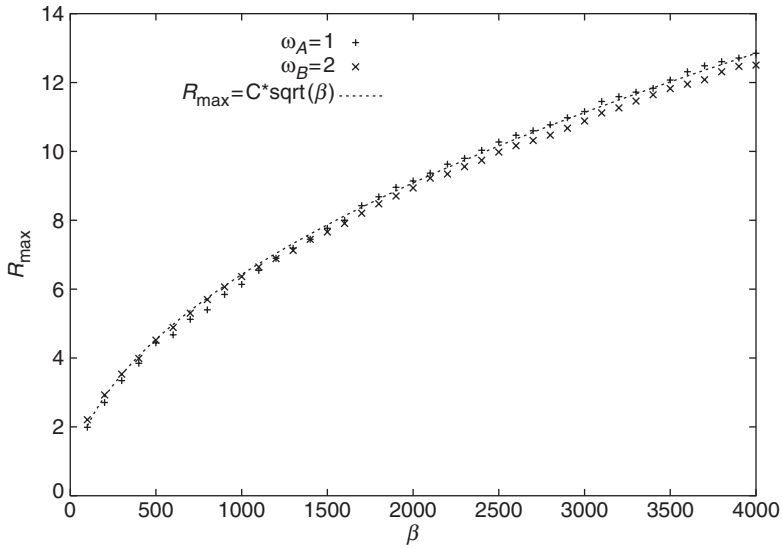

Figure 4. Graph of $R_{\max}$ vs β showing the relationship $R_{\max}^2 \sim \beta$. In all these simulations, μ is fixed at 100. At these values of β and μ, the vorticity profile of both layers are nearly uniform (flat top).

cyclonic gyre, and the cold air reservoir for potential vorticity anomaly. In short, the doubly canonical Gibbs ensemble used in the DiBattista and Majda model is optimal for the modelling of the most probable localised response of a stratified rotating flow interacting with a heat bath and an angular momentum reservoir simultaneously.

6. Negative β

For negative β, the highest attainable energy configuration is for all the vortices to clump together, forming a singularity at the origin. This is also true for the case when $\beta = 0$.

However when

$$\beta > -\frac{8\pi}{N \max\{\omega_A, \omega_B\}},$$

the partition function $Z(N)$ still remains finite, and hence the probability measure 7 is still valid. Therefore the equilibrium vortex configuration would still have a finite (non-zero) extent.

6.1. *Barotropic flow*

Figures 5 and 6 show the mean vortex density and a typical vortex distribution of a barotropic MC simulation with $N = 80$, $\mu = 1$ and $\beta = -0.1$. In this run the vortex strengths $\omega_A = \omega_B = 1$. As expected both species have the same radial profile. A Gaussian plot for $\beta = 0$ is included for comparison. When β is negative, the vortex density profile is

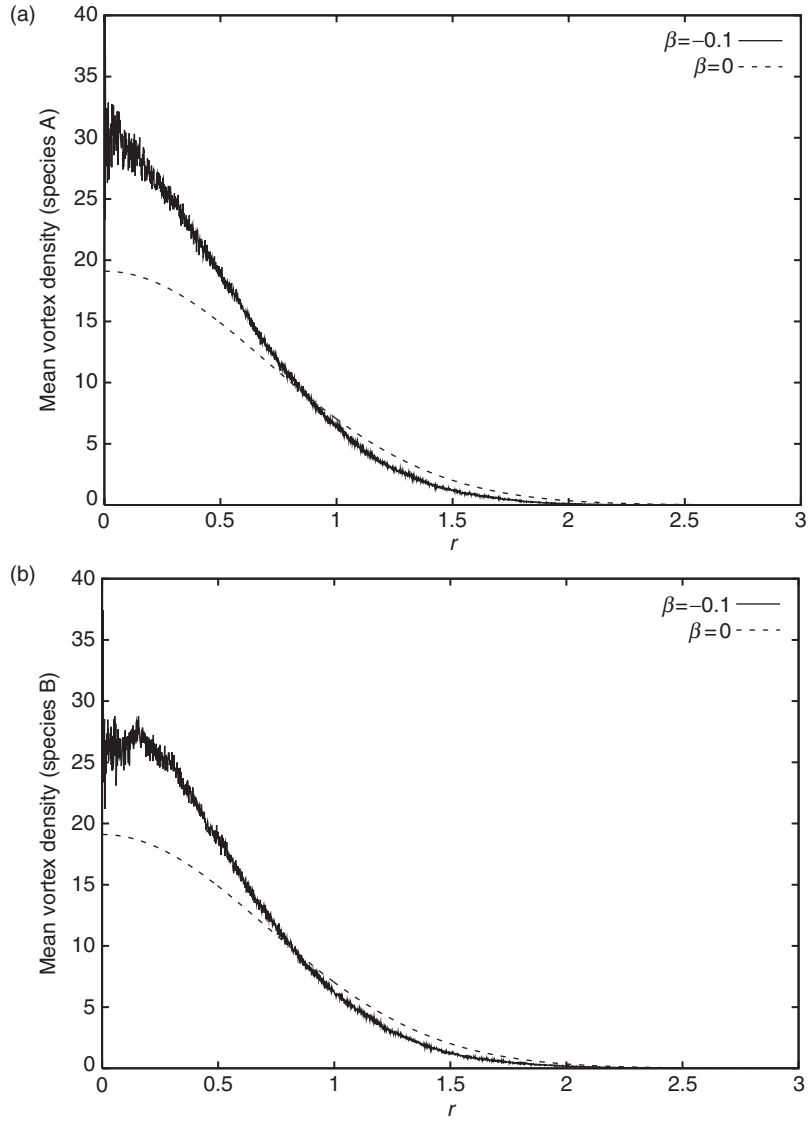

Figure 5. Mean vortex density of 80 vortices per species, with a negative $\beta = -0.1$ and $\mu = 1$. Both species have the same vorticity, $\omega_A = \omega_B = 1$. The dotted lines gives the Gaussian solution when $\beta = 0$. Kurtosis of $A = 3.1488$ and kurtosis of $B = 3.2352$.

more concentrated in the central region compared to the Gaussian. This is also reflected in the kurtosis of the density profile which is greater than three.

The simulation was carried out for two million sweeps and took about 12000 s.

420

6.2. *Baroclinic flow*

Figures 7 and 8 show the mean vortex density and a typical vortex distribution of a baroclinic MC simulation with the same parameters as before: $N = 80$, $\mu = 1$ and

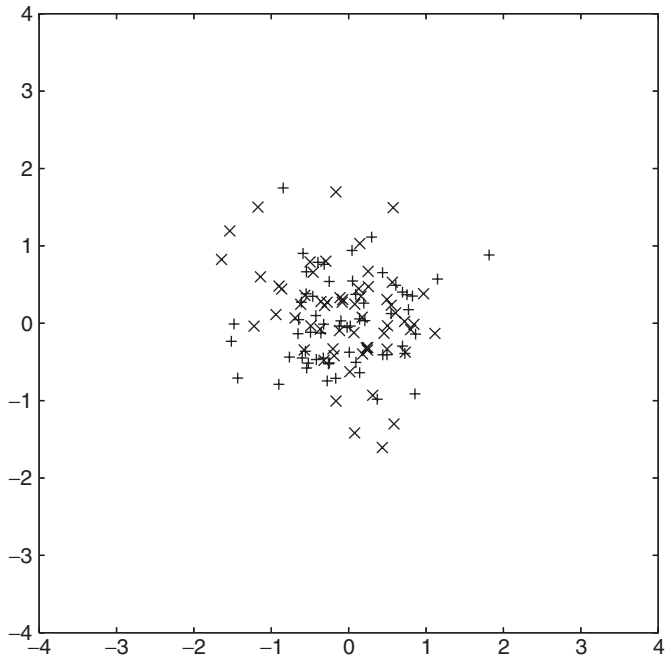

Figure 6. The distribution of 160 vortices with $\mu = 1$ and a negative $\beta = -0.1$ after 2 million sweeps. Both species have the same vorticity, $\omega_A = \omega_B = 1$.

$\beta = -0.1$. But in this run we have $\omega_A = 1$ and $\omega_B = 2$. The vortices of both species become more concentrated near the origin as ω_B increases.

In the regime

$$\beta < -\frac{8\pi}{N \max\{\omega_A, \omega_B\}},$$

the partition function is not well defined. However, we can still do MC runs with such large negative β; after all its just a matter of changing a variable for the computer simulation. And knowing that the system will be ill-behaved, the result should not be taken too seriously. If we insist on doing so, we get a vortex configuration with all the vortices moving closer and closer together until the simulation reaches the total number of sweeps or until the simulation breaks down due to a large negative energy that is beyond the computer's capability to handle.

Recall that the inverse temperature is proportional to the derivative of entropy with energy, and the more negative T is, the less hot it is. In statistical mechanics at negative temperatures, it is the maxima of the free energy of the system, $F = E - TS$ that determines the most probable state; in other words, the most probable state usually corresponds to a state of maximum entropy, whether the temperature is positive or negative. But under certain conditions, this most probable state is close to maxima of the energy E. We have seen that for low positive temperatures, this approximation principle holds in the Onsager Point Vortex gas, and it is expected to be valid also for the rotating two-layer vortex gas at low positive temperatures.

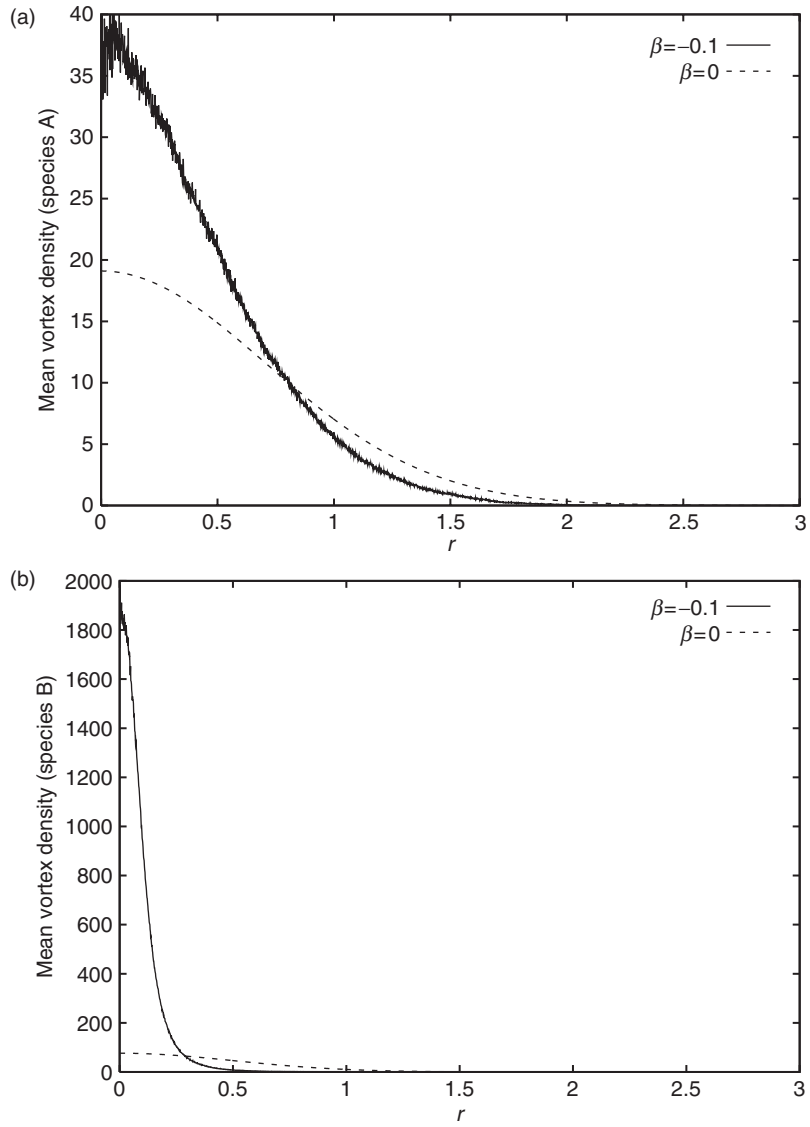

Figure 7. Mean vortex density of 60 vortices per species with a negative $\beta = -0.1$ and $\mu = 1$; $\omega_A = 1$ and $\omega_B = 2$. The dotted lines gives the Gaussian solution when $\beta = 0$. Kurtosis of $A = 3.3507$ and kurtosis of $B = 11.455$. A two-fold difference in ω causes a large 50 times difference in the vortex concentration at the centre.

This situation arises near the singularity at extremal negative temperature T_0: the distribution of vortices all lumped together near the singularity has very low entropy
445 S, but extremely high energy; any other macrostate will have larger entropy but smaller energy, leading to a smaller free energy, because the extremal temperature T_0 has the smallest allowed numerical value when it is negative. Moreover, its temperature T_0 being negative and of the smallest allowed numerical value means that the derivative of entropy with respect to the energy is negative, and a decrease of energy will lead

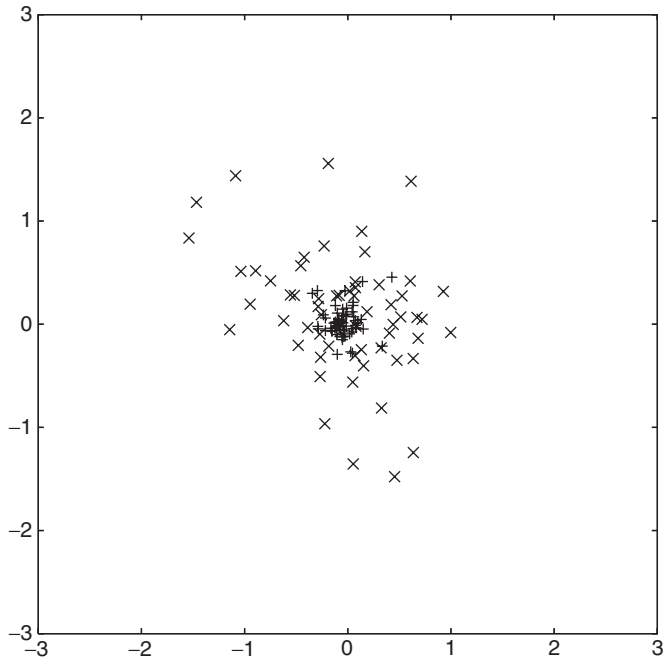

Figure 8. The distribution of 120 vortices with $\mu = 1$ and a negative $\beta = -0.1$ after 2 million sweeps. Species A ('×') has vorticity $\omega_A = 1$ while for species B ('+'), $\omega_B = 2$. The '+' vortices are more highly concentrated in the central region.

to the largest corresponding increase of entropy for a neighbouring macrostate at a slightly more negative value for T. Thus, for negative temperatures which have large numerical values, the energy of the most probable state must decrease as the entropy increases, and the approximation principle is not valid.

The simulation results in this section support the above scenario of a continuous change from the energy dominated state at the extreme negative temperature to a balanced combination of higher entropy and lower energy states at negative temperatures with large numerical values.

We do not have a finite temperature cutoff for positive temperatures, and the above approximation principle holds for different reasons than here. At very low positive temperatures, minimisers of the free energy are identical to minimisers of internal energy but they are also entropy maximisers since these macrostates are essentially radial uniform states. As the positive temperature increases, the minimisers of the free energy shifts continuously towards the Gaussian profiles which have lower entropy and higher energy. The numerical results on the rotating two-layer Gas at positive temperatures in sections 4 and 5 support this overall picture.

7. Conclusion

The approach and results in this article can be viewed from two different but related points of view. First, in view of the fact that a complete proof of the asymptotic

exactness of the mean field equations (in DiBattista and Majda 2001) is not yet available (although there should be no problem supplying one), we go behind the scene of these mean field equations and work with the ensemble of particles in the rotating two-layer model. The second point of view is to take the mean field equations as given and our approach then offers a very fast and efficient numerical method to solve these non-linear elliptic PDEs.

We conclude with a few specific physical points which are worth following up in future works. They are:

(A) As the vortex strength of species B gets progressively larger with respect to species A (cf. figure 2), the equilibrium distributions of both species become closer to a flat-top radial distribution.

(B) For any fixed ratio of vortex strengths that is not too extreme, the simultaneous appearance of both canonical types of vorticity distributions at a single positive temperature is remarkable. By canonical types we refer to the two main types of equilibrium vorticity distributions in the Onsager vortex gas on an unbounded plane, namely, the Gaussian-like radial distribution for relatively low values of β and the nearly flat-top radial distribution at higher values of β. In the Onsager vortex gas as well as in its exact mean field theory, the Gaussian type was found analytically, but the flat-top type was discovered in numerical solutions of the mean field equations (Assad and Lim 2005). A rigorous energy variational formulation for the flat-top radial solutions within a low temperature approximation to the mean field equations for the Onsager vortex gas is given in Lim and Assad (2005). This approximation is based on the idea that at low positive temperatures, the Helmholtz Free energy, $F = E - TS$, is dominated by the augmented internal energy E.

(C) For any fixed vortex strength ratio, the radial profiles of both species tend towards the flat-top uniform one as the positive inverse temperature increases.

(D) The power law of the radii of vorticity supports suggests that they are proportional to the square root of the product of the respective circulations with the ratio of inverse temperature to chemical potential

$$R \sim \sqrt{\beta\omega/\mu}.$$

As a direct result, this extended power law for the radii allows us to simulate the rotating two-layer statistics in any disk, at all values of the energy and total circulations, provided we are free to choose the chemical potential.

(E) The rigorous proof of such a power law (at least for low positive temperatures) can be constructed by minimising an augmented energy functional, along the same lines as the proof in the Onsager Vortex Gas Problem. Similar to that proof, this will likely require a technical lemma on the existence of radially symmetric and compactly supported minimisers of the augmented energy functional. One should be able to prove such a lemma using techniques from the Direct Method of the Calculus of Variations.

(F) In a restricted sense discussed in the introduction, this power law confirms that in a preconditioned barotropic gyre with sufficiently strong cyclonic signature, the baroclinic cooling is localised in an unbounded open ocean. Moreover, since the Froude numbers are small in our simulations, this cold baroclinic core is radially symmetric and concentric (with respect to the two layers), consistent with the mean field results (in DiBattista and Majda 2000). This power law with exponent 1/2 in

the quantity β/μ extends the relationship that DiBattista and Majda found between L_A and angular momentum, to the $\beta > 0$ region. Through the power law's dependence on total circulations, inverse temperature β and chemical potential μ, we are able to predict the radial extent of the equilibrium cold temperature and potential vorticity anomalies as a function of the mean kinetic energy and mean baroclinic angular momentum in the localised open ocean convection site. These quantities can be related back to the meteorological conditions that preconditioned the ocean site, such as the wind stress that caused the cyclonic gyre, and the cold air reservoir for potential vorticity anomaly.

(G) As discussed earlier, the Metropolis algorithm we used simulates this statistical interaction between the baroclinic flow and the heat and angular momentum reservoirs through prescribed values of the temperature and chemical potential. It captures the baroclinic system's robust relaxation to the unique statistical equilibrium which consists of a smooth radially symmetric vorticity distribution in each of the two layers. This coarse-grained macrostate is also the ground state which has minimal augmented energy.

However, non-equilibrium properties of the rotating two-layer model such as quasi-steady clustered vortex states are beyond the scope of the MC method in this article. Numerical simulations (and experiments) in several works (Gryanik 1983, Hogg and Stommel 1985a,b, Legg and Marshall 1993, Held *et al*. 1995, Legg *et al*. 1996, Legg and Marshall 1998, Marshall and Schott 1999) show that a strong enough barotropic rim current can suppress baroclinic instabilities in the dynamics and non-equilibrium statistical physics of a rotating stratified system, and motivate further work on a statistical dynamics approach to the interesting problem of quasi-steady clusters of two-layer vortices.

Acknowledgements

We thank anonymous referees for helpful comments on an earlier version of this paper. The work of Professor Chjan C. Lim was partially supported by ARO grant # W911NF-05-1-0001 and DOE grant # DE-FG02-04ER25616.

References

Assad, S.M. and Lim, C.C., Statistical equilibrium of the Coulomb/vortex gas on the unbounded 2-dimensional plane. *Discrete Contin. Dyn. Syst. Ser. B*, 2005, **5**, 1–14.

DiBattista, M.T. and Majda, A.J., An equilibrium statistical theory for large-scale features of open-ocean convection. *J. Phys. Oceanogr*., 2000, **30**, 1325–1353.

DiBattista, M.T. and Majda, A.J., Equilibrium statistical predictions for baroclinic vortices: The role of angular momentum. *Theor. Comput. Fluid Dyn*., 2001, **14**, 293–322.

Gryanik, V., Dynamics of localized vortex perturbations — "vortex charges" in a baroclinic fluid. *Isvestiya Atmos. and Oceanic Phys*., 1983, **19**, 347–352.

Held, I., Pierrehumbert, R., Garner, S. and Swanson, K., Surface quasi-geostrophic dynamics. *J. Fluid Mech*., 1995, **282**, 1–20.

Hogg, N. and Stommel, H., The Heton: An elementary interaction between discrete baroclinic vortices, and its implication concerning eddy heat flow. *Proc. Roy. Soc. Lond*., 1985a, **A397**, 1–20.

Hogg, N. and Stommel, H., Hetonic explosions: The breakup and spread of warm pools as explained by baroclinic point vortices. *J. Atmos. Sci*., 1985b, **42**, 1465–1476.

Legg, S. and Marshall, J., A Heton model of the spreading phase of open ocean deep convection. *J. Phys. Oceanogr*., 1993, **23**, 1046–1056.

Legg, S. and Marshall, J., The influence of the ambient flow on the spreading of convective water masses. *J. Mar. Res.*, 1998, **56**, 107–139.

Legg, S., Jones, H. and Visbeck, M., A Heton perspective of baroclinic eddy transfer in localized ocean deep convection. *J. Phys. Oceanogr.*, 1996, **26**, 2251–2266.

Lim, C.C. and Assad, S.M., Self containment radius for rotating planar flows, single-signed vortex gas and electron plasma. *Regul. Chaotic Dyn.*, 2005, **10**, 239–255.

Lim, C.C. and Majda, A.J., Point vortex dynamics for coupled surface/interior qg and propagating Heton clusters in models for ocean convection. *Geophys. Astrophys. Fluid Dyn.*, 2001, **94**, 177–220.

Lim, C.C. and Nebus, J., The spherical model of logarithmic potentials as examined by Monte Carlo methods. *Phys. Fluids*, 2004, **16**, 4020–4027.

Marshall, J. and Schott, F., Open-ocean convection: Observations, theory and models. *Rev. Geophys.*, 1999, **37**, 1–64.